PNAS RESEARCH ARTICLE | NEUROSCIENCE

STING mediates neurodegeneration and neuroinflammation in nigrostriatal α-synucleinopathy

Jared T. Hinkle[a,b,c], Jaimin Patel[b,c], Nikhil Panicker[b,c], Senthilkumar S. Karuppagounder[b,c], Devanik Biswas[b,c], Bonn Belingon[b,c], Rong Chen[b,c], Saurav Brahmachari[b,c], Olga Pletnikova[d], Juan C. Troncoso[c,d], Valina L. Dawson[a,b,c,e,1], and Ted M. Dawson[a,b,c,d,f,1]

Edited by Anders Björklund, Lund University, Lund, Sweden; received October 13, 2021; accepted February 6, 2022

In idiopathic Parkinson's disease (PD), pathologic αSyn aggregates drive oxidative and nitrative stress that may cause genomic and mitochondrial DNA damage. These events are associated with activation of the cyclic GMP-AMP synthase (cGAS)/stimulator of interferon genes (STING) immune pathway, but it is not known whether STING is activated in or contributes to α-synucleinopathies. Herein, we used primary cell cultures and the intrastriatal αSyn preformed fibril (αSyn-PFF) mouse model of PD to demonstrate that αSyn pathology causes STING-dependent neuroinflammation and dopaminergic neurodegeneration. In microglia-astrocyte cultures, αSyn-PFFs induced DNA double-strand break (DSB) damage response signaling (γH2A.X), as well as TBK1 activation that was blocked by STING inhibition. In the αSyn-PFF mouse model, we similarly observed TBK1 activation and increased γH2A.X within striatal microglia prior to the onset of dopaminergic neurodegeneration. Using STING-deficient ($Sting^{gt}$) mice, we demonstrated that striatal interferon activation in the α-Syn PFF model is STING-dependent. Furthermore, $Sting^{gt}$ mice were protected from α-Syn PFF-induced motor deficits, pathologic αSyn accumulation, and dopaminergic neuron loss. We also observed upregulation of STING protein in the substantia nigra pars compacta (SNpc) of human PD patients that correlated significantly with pathologic αSyn accumulation. STING was similarly upregulated in microglia cultures treated with αSyn-PFFs, which primed the pathway to mount stronger interferon responses when exposed to a STING agonist. Our results suggest that microglial STING activation contributes to both the neuroinflammation and neurodegeneration arising from α-synucleinopathies, including PD.

STING | Parkinson's disease | neurodegeneration | inflammation | alpha-synuclein

In idiopathic Parkinson's disease (PD), dopaminergic neurons of the substantia nigra pars compacta (SNpc) progressively degenerate within a milieu of α-synuclein (αSyn) proteopathy, neuroinflammation, and reactive gliosis (1–3). These phenomena are increasingly appreciated to be interdependent and not wholly dissociable from each other in their relationships to neurodegeneration in PD. Ordered, insoluble, and fibrillar species of αSyn protein template further aggregation of endogenous αSyn, catalyzing the spread of α-synucleinopathy throughout neural circuits (4, 5). In the process, αSyn aggregates disperse toxic oligomeric forms throughout the synaptic, axonal, and somatic cellular compartments (6, 7). These oligomers are understood to interfere with a host of normal cellular processes critical for neuronal viability, including proteostasis, mitochondrial activity, and DNA integrity and repair (8). Furthermore, αSyn aggregates engage both innate and adaptive immune processes, similar to classic pathogen-associated molecular patterns (PAMPs) (9–13). Therefore, neuroinflammation in PD and other α-synucleinopathies is not merely an epiphenomenon of neuronal damage but rather intrinsically linked to αSyn pathology.

Current research at the intersection of immunity and neurodegeneration in PD is focused on identifying the upstream signaling mechanisms that drive damaging chronic neuroinflammation. Recent studies implicate classic pattern recognition receptor (PRR)-based mechanisms, such as toll-like receptor (TLR) and nucleotide-binding oligomerization domain-like receptor (NLR) signaling, as mediators of inflammation in α-synucleinopathies (9–11, 14, 15). A distinct element of innate immunity not previously investigated in relationship to αSyn pathology is the cyclic GMP-AMP synthase (cGAS) sensor of cytosolic double-stranded DNA (dsDNA) and its mediator, stimulator of interferon genes (STING) (16, 17). The cGAS/STING system initiates an inflammatory antiviral program through both type-I interferon (IFN-I) and nuclear factor kappa-light-chain-enhancer of activated B cells (NF-κB) signaling (18, 19). cGAS/STING has been extensively studied in the context of cytosolic viral or mitochondrial DNA (mtDNA); however, genomic self-DNA also activates cGAS/STING aberrantly in the context of nuclear dysfunction, particularly when micronucleation

Significance

It is increasingly recognized that chronic neuroinflammation is causally relevant to neurodegeneration. In Parkinson's disease (PD), α-synuclein pathology activates inflammatory signaling that disturbs parenchymal homeostasis and disrupts neuron-glia interactions. Herein, we report that the innate immune cyclic GMP-AMP synthase (cGAS)/stimulator of interferon genes (STING) DNA-sensing pathway is activated in a mouse model of α-synucleinopathy and parkinsonism, leading to type-I interferon activation that precedes the onset of neurodegeneration. Remarkably, STING-deficient mice were protected from dopaminergic neuron loss in this model. We also show that αSyn aggregates can increase STING expression and augment canonical STING activation, suggesting a possible generalized propensity for exaggerated antiviral responses in neurological states with STING elevation. Our results suggest that STING inhibition may be therapeutic in idiopathic PD and possibly other human α-synucleinopathies.

The authors declare no competing interest.

This article is a PNAS Direct Submission.

Copyright © 2022 the Author(s). Published by PNAS. This article is distributed under Creative Commons Attribution-NonCommercial-NoDerivatives License 4.0 (CC BY-NC-ND).

See online for related content such as Commentaries.

[1]To whom correspondence may be addressed. Email: tdawson@jhmi.edu or vdawson@jhmi.edu.

This article contains supporting information online at http://www.pnas.org/lookup/suppl/doi:10.1073/pnas.2118819119/-/DCSupplemental.

Published April 8, 2022.

and DNA breaks are present (20–24). In neurons, αSyn aggregates cause DSBs in genomic DNA due to increased nitrative stress (25), suggesting a connection between DNA damage and α-synucleinopathies. However, it is not currently known whether αSyn aggregation is capable of driving cGAS/STING-dependent neuroinflammation that contributes to neurodegeneration in PD.

In the present work, we used primary mouse cell cultures and the intrastriatal αSyn preformed fibril (αSyn-PFF) mouse model of PD (5) to examine whether cGAS/STING activation is a consequence of pathologic αSyn aggregation. We report that αSyn aggregates cause DSBs in microglial DNA and STING-dependent microglial inflammation that occurs prior to the onset of neurodegeneration. Furthermore, STING knockout was neuroprotective in the αSyn-PFF model, reducing inflammation, motor deficits, αSyn pathology, and SNpc neuron degeneration. STING was up-regulated in the SNpc of human PD patients and primed for maximal activation in primary microglia treated with αSyn-PFFs. These results suggest that cGAS/STING activation may exacerbate pathologic neuroinflammation in α-synucleinopathies such as idiopathic PD.

Results

αSyn-PFFs Cause Glial Genotoxicity and cGAS/STING Activation In Vitro. To determine potential cellular sources of cGAS/STING activation, we examined cytoplasmic expression of pathway components in primary mouse cell cultures treated with αSyn-PFF (Fig. 1*A*). In primary neuronal cultures, we detected no STING expression and little or no expression of cGAS or their effector TBK1. By contrast, STING was strongly expressed in mixed glial cultures enriched for microglia and astrocytes (MA cultures). Therefore, we investigated whether αSyn-PFFs induce genotoxic stress or cGAS/STING activation in MA cultures. We found increased Ser139-phosphorylated H2A.X (γH2A.X), a marker of DSBs (26), in MA cultures after 24 h of αSyn-PFF treatment (Fig. 1 *B* and *D* and *SI Appendix*, Fig. S1*A*). This time course aligned with accumulation of Ser172-phosphorylated TBK1 (pTBK1) in noncytoplasmic cell fractions (*SI Appendix*, Fig. S1*A*), reflecting relocalization to lipid rafts at the trans-Golgi network (27, 28). H-151, a selective inhibitor of STING activation, blocked the appearance of pTBK1 in the MA cultures (Fig. 1 *C* and *E*), suggesting that TBK1 auto-phosphorylates in a STING-dependent manner. Notably, αSyn-PFFs caused a significant increase in the cGAS product and STING activator 2′3′-cGAMP (Fig. 1*F*) of MA cultures, further suggesting canonical cGAS/STING activation. In separate experiments with microglia-depleted cultures, this pattern was not observed, suggesting that microglia are important for STING activation in vitro (*SI Appendix*, Fig. S1*B*).

Striatal Interferon Induction in the αSyn-PFF Mouse Model of PD Is STING-Dependent. Given our observation that αSyn-PFFs caused nuclear DSBs and cGAS/STING activation in vitro, we next investigated whether this occurs in vivo. In the αSyn-PFF mouse model of PD (5), microglial activation and reactive astrogliosis precede and accompany the dopaminergic SNpc neurodegeneration that is reliably observed after 6 mo postinjection (14, 29, 30). Therefore, we investigated whether DNA damage and cGAS/STING activation may contribute to neuroinflammation related to α-synucleinopathy in the PFF model. We focused on microglia, which are the principal immune cells of the CNS and were previously shown to be the main cell type expressing STING in the CNS (31, 32). At 3 mo after bilateral striatal αSyn-PFF injection, prior to the onset of SNpc degeneration, we observed a substantial and significant increase in the number of pTBK1$^+$ cells in the striatum (Fig. 2 *A* and *B*). Notably, pTBK1 intensity was increased in both Iba1$^+$ and Iba1$^-$ cells, suggesting that α-synucleinopathy activates pTBK1 via multiple cellular mechanisms. The relative area of Iba1$^+$ signal that colocalized with pTBK1 was also significantly increased in the αSyn-PFF group (Fig. 2*B*), indicating a larger proportion of microglia with activated TBK1. We also found that the PFF-injected mice had significantly increased nuclear or peri-nuclear γH2A.X foci in the striatum (Fig. 2 *C* and *D* and *SI Appendix*, Movies S1 and S2) at 3 mo after bilateral striatal injection. Furthermore, this evidence of genomic DNA damage was highly concentrated in microglia as indicated by the increased amount of Iba1$^+$ cells with γH2A.X expression (Fig. 2*D* and *SI Appendix*, Movies S3 and S4). The nuclear and perinuclear localization of γH2A.X may both reflect formation of micronuclei, which have previously been shown to associate with both cGAS and γH2A.X (20, 33).

Because our results suggested that α-synucleinopathy induces DNA DSBs in microglia in vitro and in vivo, we next tested the mechanistic hypothesis that this causes cGAS/STING-

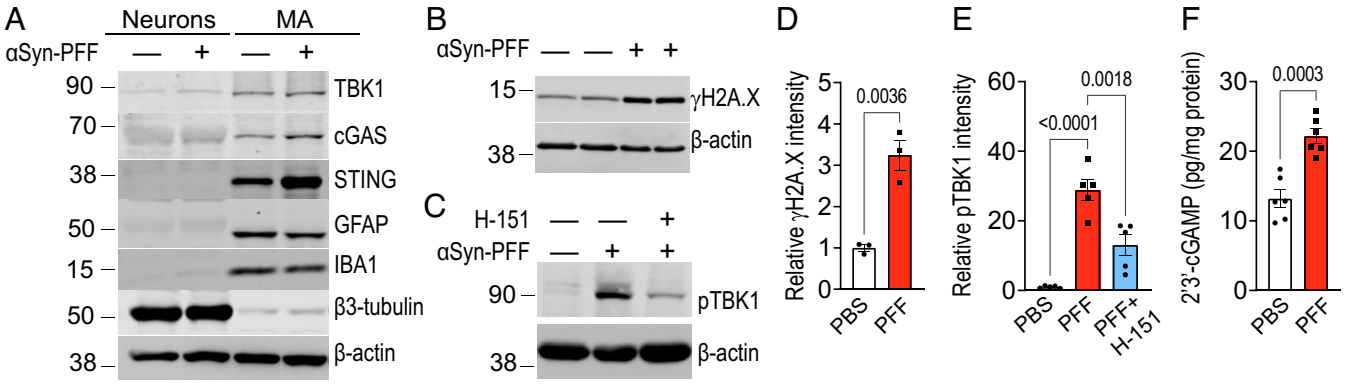

Fig. 1. αSyn-PFFs cause glial genotoxicity and cGAS/STING activation in vitro. (*A*) Representative Western blot analysis of cytoplasmic (Triton X-100 soluble) cell fractions isolated from primary cerebrocortical cultures of mouse neurons or mixed cultures of microglia and astrocytes (MA) treated with PBS vehicle or α-synuclein preformed fibrils (αSyn-PFF) for 24 h. (*B*) Representative Western blot analysis of the DNA double-strand break marker γH2A.X in MA glial cultures treated as in (*A*). (*C*) Representative Western blot of pTBK1 in noncytoplasmic fractions (Triton X-100 insoluble) of MA cultures treated for 24 h with PBS vehicle or αSyn-PFF ± STING inhibitor H-151 (5 μM). (*D*, *E*) Quantifications of actin-normalized γH2A.X band intensity from B ($n = 3$) or pTBK1 band intensity from *C* ($n = 5$). *P* value from two-tailed *t* test ($t = 6.13$, $df = 4$) in *D* and from one-way ANOVA with Tukey post hoc comparisons in *E* (PBS vs. PFF: $q = 11.32$; PFF vs. PFF+H151: $q = 6.42$; $df = 12$). (*F*) Enzyme-linked immunosorbent assay (ELISA) for the cGAS activation product and STING ligand 2′3′-cyclic-GMP-AMP (cGAMP) in MA glial cultures treated with PBS vehicle or αSyn-PFF for 24 h ($n = 6$). *P* value from two-tailed *t* test ($t = 5.43$, $df = 10$).

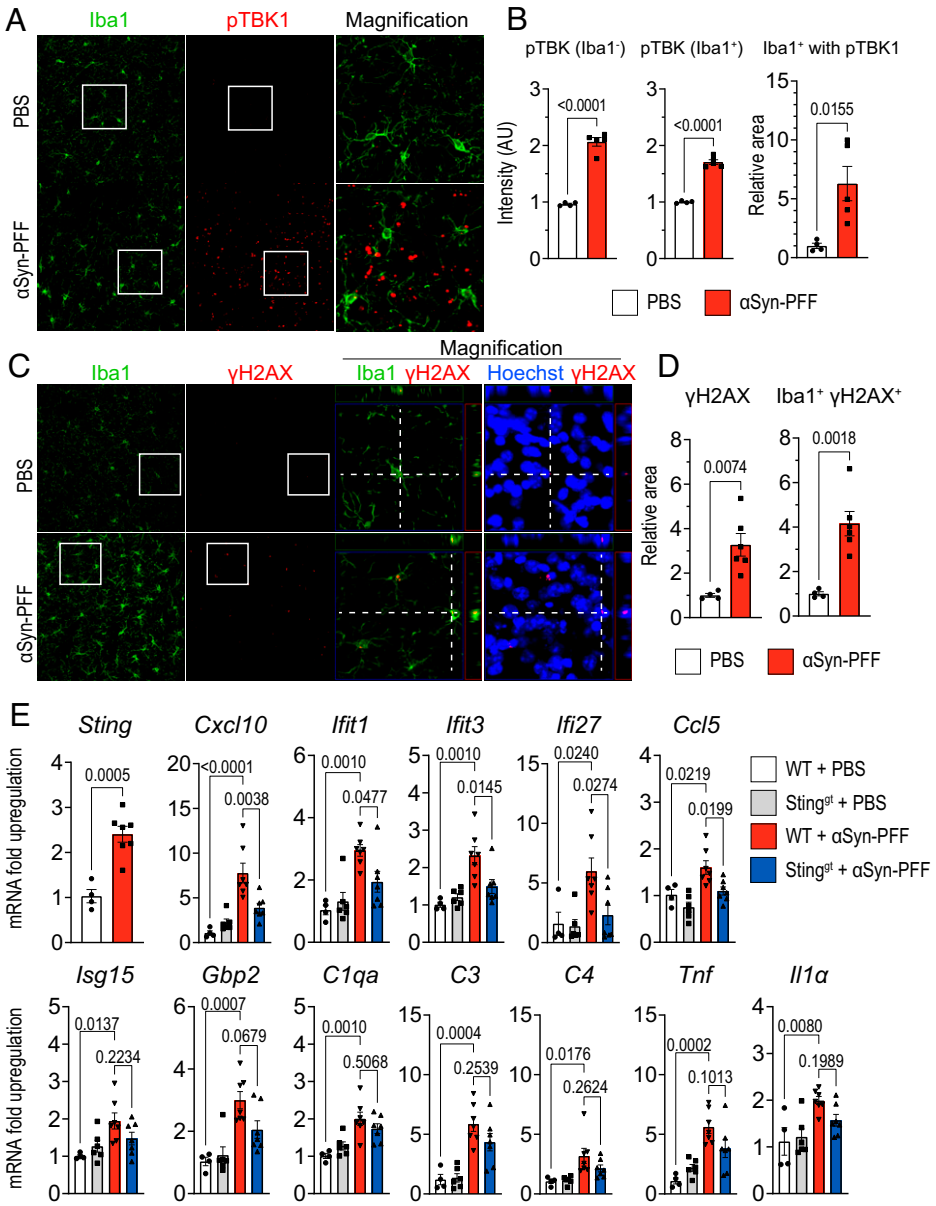

Fig. 2. Striatal α-synucleinopathy causes microglial DNA damage and STING-dependent interferon induction. (*A*) Representative immunofluorescence staining for striatal pTBK1 in tissues prepared from WT mice 3 mo after bilateral striatal injection with αSyn-PFF. (*B*) Quantification of the signal intensity for pTBK1 in microglia (Iba1^{+}) or nonmicroglial (Iba1^{-}) cells of the striatum and the total microglial pTBK1 as measured by the proportion of Iba1 signal with colocalized pTBK1. All data are mean ± SEM. *P* values from unpaired *t* tests (pTBK Iba1^{-}: $t = 12.65$; pTBK Iba1^{+}: t = 14.8; Iba1^{+} proportion pTBK^{+}: $t = 3.18$, all $df = 7$). (*C*) Representative immunofluorescence staining with orthogonal Z-stack views for striatal γH2A.X in tissues prepared from WT mice 3 mo after bilateral striatal injection with αSyn-PFF. (*D*) Quantification of the total nuclear (Hoechst^{+}) and microglial (Iba1^{+}) γH2A.X measured by the proportion with colocalized γH2A.X. All data are mean ± SEM *P* values from unpaired *t* tests (γH2A.X: $t = 3.56$; Iba1^{+} γH2A.X: $t = 4.59$, all $df = 8$). (*E*) qPCR was used to measure transcription of *Sting* and inflammatory markers in striatal tissue of WT or Sting^{gt} mice 3 mo after unilateral striatal injection with αSyn-PFF or PBS vehicle. All data are mean ± SEM *P* values from unpaired *t* test for *Sting* upregulation in WT mice injected with PFF ($t = 5.27$, $df = 9$) and two-way ANOVA with Tukey post hoc multiple comparisons tests for all other targets (test statistics in *SI Appendix*, Dataset S1).

dependent neuroinflammation. The intrastriatal αSyn-PFF experiment was repeated with a comparison group of Goldenticket mice (Sting^{gt}) mice, which lack STING protein due to a mutant missense allele in *Sting* (34). qPCR was then used to characterize the induction of inflammatory genes. In wild-type (WT) mice, unilateral αSyn-PFF injection increased transcription of *Sting* in the ipsilateral striatum after 3 mo, suggesting the pathway might be primed for activation prior to SNpc degeneration (Fig. 2*E*). Consistent with this idea, WT mice injected with αSyn-PFF exhibited upregulation of several interferon signaling genes associated with cGAS/STING activation, such as *Cxcl10*, *Ifit1*, *Ifit3*, and *Ifi27* (Fig. 2*E*). We observed significant reduction of this interferon response in Sting^{gt} mice, suggesting that STING mediates striatal interferon activation in the αSyn-PFF model. Interestingly, rescue of complement gene transcription (*C1qa*, *C3*, and *C4*) and common inflammatory markers (e.g., *Tnf*, *Il1a*) were relatively attenuated and not statistically significant, suggesting that striatal STING signaling is predominantly associated with interferon activation at 3 mo postinjection.

STING Knockout Is Neuroprotective in the αSyn-PFF Model. To determine whether reducing cGAS/STING activation may ameliorate nigrostriatal dysfunction and dopaminergic neurodegeneration secondary to αSyn proteopathy, we examined behavioral and biochemical markers of PD-like deficits in WT

and Sting^{gt} mice injected in bilateral striatum with αSyn-PFFs. At 9 mo postinjection, WT mice exhibited motor deficits on the accelerating rotarod, grip strength test, and pole test (Fig. 3 *A*–*C*). These deficits were not observed in the Sting^{gt} mice (Fig. 3 *A*–*C*), suggesting that these mice are protected from motor deficits in the αSyn-PFF model. Immunohistochemical analysis of SNpc brain sections from these mice indicated that αSyn-PFFs induced dopaminergic SNpc neurodegeneration in the WT mice that was attenuated in the Sting^{gt} group (Fig. 3 *D*–*F*). Relative to WT mice, there was also a significant reduction in pathologic phosphorylated αSyn (pS129-αSyn) in SNpc dopaminergic neurons of the Sting^{gt} mice (Fig. 3 *G* and *H*). Finally, in the striatum, WT αSyn-PFF mice exhibited a significant reduction of dopamine (Fig. 3*I*) and its metabolites homovanillic acid (HVA), 3,4-dihydroxyphenylacetic acid (DOPAC), and 3-methoxytyramine (3-MT), which was not observed in the Sting^{gt} mice (*SI Appendix*, Fig. S2). Collectively, these results indicate that STING knockout mice are generally protected from the clinico-pathologic PD-like signs that are usually observed in the αSyn-PFF model. In vitro, the STING inhibitor H-151 did not protect primary neuronal cultures from αSyn-PFF cytotoxicity (*SI Appendix*, Fig. S3), which corroborates the notion that STING-dependent neurotoxicity in the SNpc largely arises from non–cell-autonomous signaling or inflammation.

STING Is Upregulated in Human PD. To determine whether idiopathic PD exhibits increased or altered markers of the cGAS/STING pathway, we analyzed SNpc tissue from autopsied idiopathic PD patients and age-matched controls (metadata in *SI Appendix*, Table S1). Compared to controls, PD patients had significantly increased STING protein expression (Fig. 4 *A* and *B*). Interestingly, we did not observe a commensurate increase in pTBK1 in the PD tissue (Fig. 4*C*). Given that TBK1 functions in different pathways and cell types (35), the relative amount phosphorylated as part of STING activation may be relatively small in whole-tissue extracts or reduced in late disease. In support of our hypothesized connection between STING and pathologic α-synuclein aggregation, STING

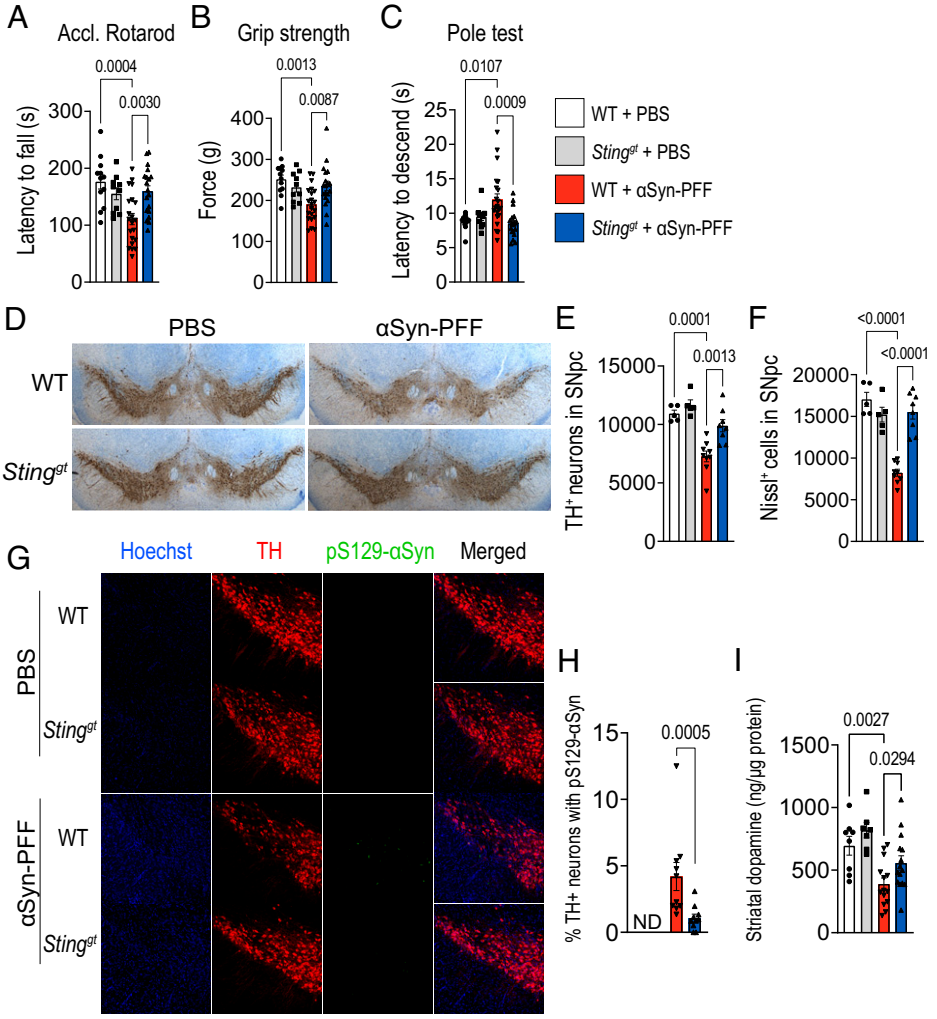

Fig. 3. STING knockout is neuroprotective in the αSyn-PFF model. (*A*–*C*) Behavioral analyses of WT and Sting^{gt} mice 9 mo after bilateral striatal injection with αSyn-PFF or PBS vehicle. Results from accelerating rotarod (*A*), grip strength test (*B*), and pole test (*C*) presented as mean ± SEM (10–21 mice per group). *P* values are derived from two-way ANOVA with Tukey post hoc comparisons (test statistics in *SI Appendix*, Dataset S2). (*D*) Representative immunohistochemistry for tyrosine hydroxylase (TH) counterstained with a thionin Nissl stain in ventral midbrain of WT and Sting^{gt} mice in fixed cryopreserved tissue sections. (*E*, *F*) Unbiased stereological counts of TH$^+$ neurons (*E*) and TH$^-$, Nissl$^+$ neurons (*F*) in the SNpc. Data are mean ± SEM *P* values from two-way ANOVA with Tukey post hoc comparisons (test statistics in *SI Appendix*, Dataset S2). (*G*) Representative immunostaining for pS129-αSyn (green) and TH (red) with Hoechst counterstain. Scale bar = 100 μm. (*H*) Quantification of the percentage of TH-positive neuronal somas with pS129-αSyn+ inclusions in the substantia nigra section with maximal pS129-αSyn+ inclusion density for each mouse (10 mice per group). ND = No pS129-αSyn+ inclusions detected. *P* value from two-tailed nonparametric Mann-Whitney test (medians: 3.25 vs. 0.92; $n = 10$; $U = 7$). (*I*) Striatal dopamine measurement by HPLC. Two-way ANOVA with Holm-Šídák post hoc multiple comparisons test ($df = 40$; $t = 3.45$ [WT-PBS vs. WT-PFF], $t = 2.26$ [WT-PFF vs. Sting^{gt}-PFF).

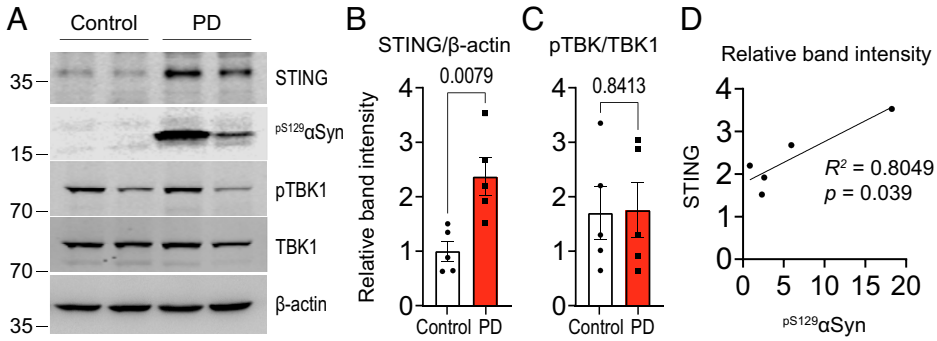

Fig. 4. STING is up-regulated in human PD. (*A*) Representative Western blot analysis of proteins in substantia nigra tissue from autopsied cases of diagnosed PD and controls. (*B*, *C*) Quantification of STING (*B*) and pTBK1 (*C*) band intensities after normalization to actin and TBK1, respectively ($n = 5$), *P* values from two-tailed nonparametric Mann-Whitney test (STING: medians 0.88, 2.20; $n = 5$; $U = 0$. pTBK1: medians 1.30, 1.29; $n = 5$; $U = 11$). (*D*) Linear regression analysis of the relationship between STING and pSer129-αSyn band intensities in (*A*), including percent explained variance (R^2) and exact *P* value.

protein level correlated significantly and linearly with the amount of pS129-αSyn among the PD tissue samples (Fig. 4*D*).

αSyn-PFFs Prime Microglial cGAS/STING for Maximal Signaling. In vitro, MA cultures stimulated with αSyn-PFFs exhibit substantial upregulation of STING protein, but much less pronounced increases in cGAS or TBK1 (Fig. 5 *A* and *B*). Modulation of STING protein expression could function as a priming mechanism for increasing the cGAS/STING pathway's sensitivity to activating stimuli. Recently, this functional outcome was observed in a mouse model of Niemann-Pick disease type C due to altered cellular trafficking that increased the amount of functional microglial STING protein (36). To determine whether αSyn-PFFs cause a similar priming effect of cGAS/STING, we treated microglia with αSyn-PFFs for 24 h as a priming signal, then used the synthetic STING agonist 5,6-dimethylxanthenone-4-acetic acid (DMXAA, also known as vadimezan) to trigger immediate STING activation (Fig. 5*C*). We found that there was a multiplicative or synergistic effect between αSyn-PFF priming and DMXAA on transcription of several key interferon-induced genes (Fig. 5*D*). This was reflected in statistically significant interaction terms in two-way ANOVA analyses for *Cxcl10*, *Ifit3*, *Ccl5*, and *Isg15* (*SI Appendix*, Table S2). We also examined whether αSyn-PFF priming led to increased cytokine secretion (in cell culture media) using enzyme-linked immunosorbent assay (ELISA). Similar to the gene transcription results, there was a synergistic relationship between αSyn-PFF priming and DMXAA in promoting the secretion of Cxcl10 protein, as well as IFNβ (Fig. 5*E* and *SI Appendix*, Table S3). Interestingly, DMXAA did not stimulate TNF secretion despite *Tnf* induction, suggesting a complex relationship between STING activation and TNF release (Fig. 5*E*). We did not observe IFNγ secretion in any condition, suggesting that these responses were not indirectly mediated by IFN-II signaling.

Discussion

The cellular and molecular biology of α-synucleinopathy strongly implicates multifactorial organelle damage as a consequence of αSyn aggregation (8). In turn, the nature of these deficits—which include nuclear dysfunction and DNA damage—strongly suggest the capacity to trigger canonical cGAS/STING activation. The studies presented here show that the cGAS/STING pathway is indeed activated and contributes to neurodegeneration in a mouse model of idiopathic PD. We also show that αSyn-PFFs cause both genomic DNA damage and cGAS/STING signaling both in vitro and in vivo, suggesting that genotoxicity may be upstream of cGAS/STING activation.

αSyn-PFF injections into the mouse striatum reliably engender αSyn pathology by initiating the templated misfolding of endogenous αSyn monomer, likely in the presynaptic compartment of nigrostriatal terminals (5). Here, we found striatal interferon activation within 3 mo of injection, which corresponds to an early stage of disease progression with minimal dopaminergic neurodegeneration and no significant motor impairment (25). Neuroinflammation has long been recognized as being a characteristic of PD and other neurodegenerative diseases, but only in the past decade or so has it become widely considered as something more than an epiphenomenon. This recognition, combined with slow progress in developing disease-modifying therapies, has prompted us to explore how the disruption of inflammatory cascades or loops might constitute a viable therapeutic strategy for blocking neurodegeneration. For example, we have previously shown that reducing microglia-derived neuroinflammation can reduce neurodegeneration and the accumulation of pathologic αSyn in neurons in the αSyn-PFF and A53T mouse models of PD (30). Other recent work has shown that activated microglia directly promote neuronal αSyn aggregation in PFF-based models (37). Reduced interferon signaling in microglia is also associated with lower Aβ aggregate propagation, suggesting that modulation of microglial phenotype is a viable therapeutic approach in neurodegeneration (38). The ideal disease-ameliorating modification of microglial function may be selective reduction in inflammatory activities that preserves adaptive phagocytic functions. Our studies suggest that reducing cGAS/STING activation may be useful in this regard.

Our findings also describe the nature of STING-dependent immune responses in PD. For example, we observed induction of chemokines such as *Cxcl10* and *Ccl5*, which are important chemokines that increase infiltration of immune cells, including lymphocytes (39). *CXCL10* was also recently found to be upregulated in striatal tissue of Huntington's diseasepatients, along with apparent activation of cGAS/STING (23). Lymphocytic infiltration and CCL5 increases were similarly observed in the nonhuman primate MPTP parkinsonism model (40), although it is not clear how directly comparable these studies are to our αSyn-PFF model study. However, T-cell infiltration into the SNpc of human PD patients has been documented and Th17 lymphocytes increase iPSC-derived midbrain neuron

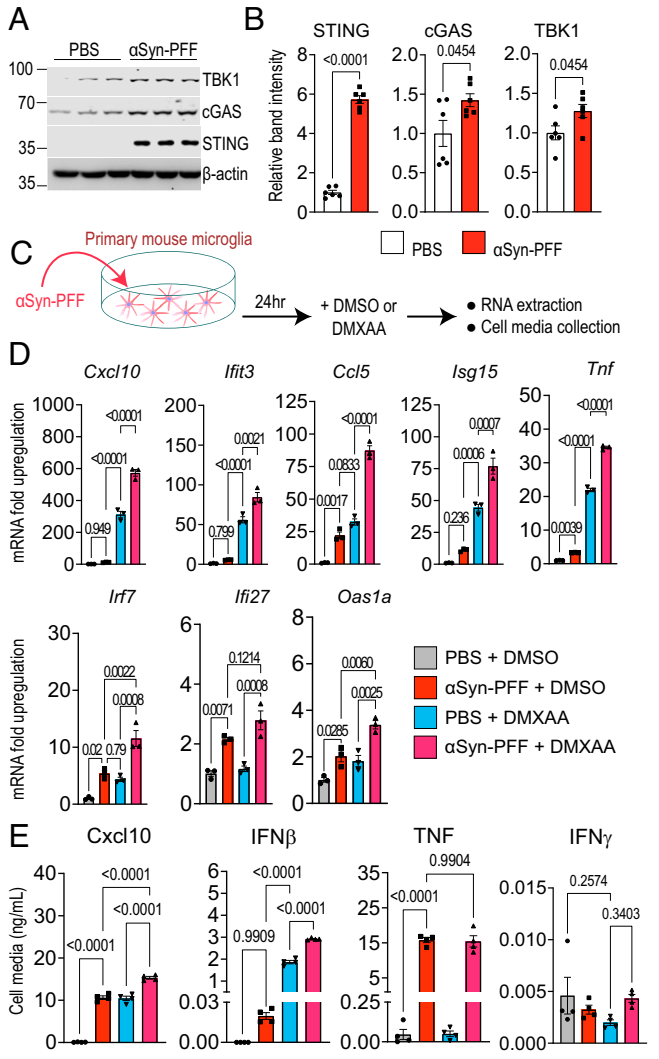

Fig. 5. αSyn-PFFs prime microglial cGAS/STING for maximal signaling. (*A*, *B*) Representative Western blots (*A*) and quantification (*B*) of cytoplasmic STING and cGAS in MA cultures treated as in *A* ($n = 6$). *P* values from two-tailed *t* tests (STING: $t = 21.2$; cGAS: $t = 2.28$; TBK1: $t = 2.29$; all $df = 10$). (*C*) Approach to test the hypothesis that STING upregulation in αSyn-PFF-treated microglia primes more potent immune responses to STING ligands. DMXAA, 5,6-dimethylxanthenone-4-acetic acid; DMSO, dimethyl sulfoxide. (*D*) qPCR was used to measure the priming of microglial interferon activation by 24 h αSyn-PFF treatment followed by a 120-min secondary treatment with the STING activator DMXAA (10 μg/mL) or vehicle (DMSO). *P* values from two-way ANOVA followed by Tukey's post hoc test (test statistics in *SI Appendix*, Dataset S3). (*E*) ELISA analysis of microglial cell culture media cytokines after pretreatment with αSyn-PFF or PBS vehicle for 24 h followed by 4 h exposure to DMSO or DMXAA (10 μg/mL) *P* values from two-way ANOVA followed by Tukey's post hoc test (test statistics in *SI Appendix*, Dataset S3).

death, suggesting a possible role for lymphocytic infiltration as a pathologic event in idiopathic PD (12). cGAS/STING also has conserved roles in autophagy induction (41); future work may clarify whether this is mechanistically important in conditions such as idiopathic PD that are marked by proteostatic dysfunction and protein aggregation.

In seeking to relate our mechanistic mouse studies to human PD, we also found that STING protein levels were upregulated in lysates of SNpc tissue isolated from human PD patients relative to age-matched controls. Interestingly, STING protein levels correlated positively with the amount of pSer129-αSyn, supporting a connection between pathologic αSyn accumulation and STING. We did not see a clear increase in the ratio of pTBK1 to TBK1 in the PD patients, though this may be related to the activity of TBK1 and its phosphorylation as part of signaling pathways other than cGAS/STING (35). For example, TBK1 is a key regulator of autophagy in both neurons and glia (42). One group reported that loss of function mutations in TBK1 can accelerate disease onset, impair autophagy, and increase SOD1 aggregation in the $SOD1^{G93A}$ ALS mouse model (43). However, point mutations that only partially reduce TBK1 kinase activity accelerated disease onset while reducing interferon activation and extending lifespan relative to full TBK1 loss. Thus, TBK1 activation is a relatively complex and dose-sensitive process that may not lead to clear changes in pTBK1 level in bulk tissue. Finally, we also note that the high degree of variability in pTBK1/TBK1 in our samples (compared to STING) may reflect biases arising from comorbid conditions and the nonspecificity of neuroinflammatory signaling to PD.

Our in vitro data suggest that the STING upregulation detected in PD tissue may be important for basal or chronic cGAS/STING-dependent inflammation. Priming microglia with αSyn-PFFs increased STING expression and amplified interferon responses elicited by the STING agonist DMXAA. An analogous mechanism that increases the amount of functional STING in microglia contributes to neurologic disease in Niemann-Pick disease (36). Increased STING expression could also theoretically reduce its activation threshold with respect to intracellular cGAMP concentrations. Finally, basal cGAS activity increases as a function of cellular senescence (21, 22, 33, 44), suggesting that increased STING expression in persons with PD could amplify the effects of inflammation on the CNS and further accelerate senescence. Normalizing or disrupting this cGAS/STING signaling may therefore be therapeutically useful for reducing damaging chronic neuroinflammation in PD.

In summary, our work demonstrates that STING is activated by the effects of αSyn aggregation in a model of idiopathic PD and that its knockout ameliorates neuroinflammation and neurodegeneration. Other recent publications have revealed pathologic STING activation in neurodegenerative disease models (23, 24, 36, 45–48), suggesting a wider significance of antiviral cGAS/STING signaling to neurologic disease. Our laboratory has also demonstrated that α-synucleinopathy causes neurodegeneration through genotoxic stress in neurons that leads to cell death via parthanatos (25, 49). The present work complements this line of research by demonstrating pathologic consequences of DNA damage in glial cells. Interventions that preserve the integrity or repair of genomic DNA may therefore be an effective upstream approach to halt pathologic processes across diverse cell types in the CNS during neurodegeneration.

Materials and Methods

Mice. C57BL/6 (WT) and "Goldenticket" (34) $Sting^{gt}$ (Jackson stock #017537) adult mice were obtained from Jackson Laboratory. CD1 mice were from Charles River. Animal usage in this project followed guidelines put forth by the Johns Hopkins University Animal Care and Use Committee (ACUC). The procedures are part of our ACUC-approved protocol, MO20M262.

Postmortem SNpc Tissue. Frozen SNpc tissue extracts from autopsied PD patients ($n = 5$) and age-matched controls ($n = 5$) were obtained from the Division of Neuropathology, Department of Pathology at Johns Hopkins School of Medicine.

Primary Cell Culture. Primary glial cerebrocortical cultures were established by dissociating tissue from P0-P2 mouse pups and plating in a growth medium (DMEM/F12 with 10% FBS, 50 U/mL penicillin, 50 μg/mL streptomycin, 2 mM L-glutamine, 100 μm nonessential amino acids, and 1 mM sodium pyruvate).

Microglia were isolated via immunomagnetic separation with the EasySep Mouse CD11b Positive Selection Kit (Stemcell Tech). Astrocytes were isolated by serial passaging as in previous work (30). Alternatively, no selection method was used to maintain mixed microglia/astrocyte cultures. Primary neuron cultures were prepared similar to previous work (30).

αSyn-PFF Preparation and Use. Recombinant mouse αSyn-PFFs were made as described previously (4) with minor modifications. PFFs were sonicated at 20% amplitude for 30 seconds (0.5s on/off) with a probe-tip sonicator (Branson Digital Sonifier, Danbury, CT). For neurotoxicity experiments, αSyn-PFFs were added to cell culture media to a final concentration of 5 μg/mL per convention. For experiments in astrocytes, microglia, or microglia-astrocyte cultures, a concentration of 2 μg/mL was used unless otherwise specified. Striatal coordinates for stereotactic injection were +0.2 mm (AP), +2 mm (ML), and +2.8 mm (DV).

Behavioral Assays. All behavioral assays were performed as previously described (25).

HPLC. Striatal biogenic amines were measured using high-performance liquid chromatography (HPLC) with electrochemical detection (ECD) as previously described (25).

Quantitative PCR. RNA was extracted from homogenized striatal tissues or cells using TRIzol reagent (Invitrogen, Waltham, MA). Total RNA was reverse transcribed to cDNA with the High Capacity cDNA Reverse Transcription Kit (Applied Biosystems, Waltham, MA). SYBR Green Master Mix (Applied Biosystems) was used for quantitative RT-PCR (qPCR) using a Viia7 Real-Time PCR System (Applied Biosystems). Primer sequences used are listed in the supplement (*SI Appendix*, Table S4).

Immunohistochemistry and Stereology. PFA-fixed cryopreserved brains were sectioned at 30 μm thickness using a sliding microtome (Microm HM 450, ThermoFisher, Waltham, MA). For SNpc cell counting studies, immunohistochemistry for tyrosine hydroxylase (TH) was performed using a VECTASTAIN Elite ABC-HRP kit (PK-6101) with rabbit anti-TH antibody from Novus Biologicals (NB300-109, 1:1,500). TH^+ neurons and TH^- neurons ($Nissl^+$) were counted in parallel using an unbiased computer-assisted stereological platform (Stereo Investigator software, MicroBrightfield, Willison, VT) connected to an Axiophot photomicroscope (Carl Zeiss) with motorized stage (Ludl Electronics) and camera (Hitachi HV C20). For immunofluorescence analyses of TH/pS129-αSyn, stained sections were imaged at equal exposure settings and total TH^+ neurons were counted for each image. $pS129\text{-}\alpha Syn^+$ and TH^+ (double-positive) cells were then counted and divided by the total number of TH^+ cells. For pTBK1 and γH2A.X analyses, images were acquired using a Zeiss LSM 880 confocal scanning microscope and quantification of colocalization or intensity was performed using the Zen software (Carl Zeiss).

ELISA. Cytokines were measured in cell culture media and detergent-soluble brain tissue fractions with DuoSet ELISA development systems (R&D Systems): mouse CXCL10/IP-10/CRG-2 (DY466); mouse IFNβ (DY8234); mouse IFN-gamma (DY485); and mouse TNF (DY410). 2′3′-cGAMP was measured using the 2′3′-cGAMP ELISA kit from Cayman Chemical (501700).

Data Availability. Correspondence and requests for materials and access to datasets should be addressed to T.M.D. and V.L.D. All study data are included in the article and/or *SI Appendix*.

ACKNOWLEDGMENTS. This work was supported by the JPB Foundation and the Farmer Family Foundation. T.M.D. is the Leonard and Madlyn Abramson Professor in Neurodegenerative Diseases. J.T.H. is supported through the Medical Scientist Training Program at Johns Hopkins University School of Medicine (NIH/NIGMS T32 GM136577) and through a predoctoral NRSA (NIH/NIA F30AG067643). N.P. was supported by a postdoctoral fellowship from the Maryland Stem Cell Research Fund (2017-MSCRFF-3838) and is currently supported by a Pathway to Independence grant from the NIA/NIH (K99AG066862). JHU Alzheimer's Disease Research Center (NIH P50AG05146) contributed postmortem brain tissues.

Author affiliations: [a]Solomon H. Snyder Department of Neuroscience, Johns Hopkins University School of Medicine, Baltimore, MD 21205; [b]Neuroregeneration and Stem Cell Programs, Institute for Cell Engineering, Johns Hopkins University School of Medicine, Baltimore, MD 21205; [c]Department of Neurology, Johns Hopkins University School of Medicine, Baltimore, MD 21205; [d]Department of Pathology, Johns Hopkins University School of Medicine, Baltimore, MD 21205; [e]Department of Physiology, Johns Hopkins University School of Medicine, Baltimore, MD 21205; and [f]Department of Pharmacology and Molecular Sciences, Johns Hopkins University School of Medicine, Baltimore, MD 21205

Author contributions: J.T.H., V.M.D., and T.M.D. designed research; J.T.H., J.P., N.P., S.S.K., D.B., B.B., R.C., and S.B. performed research; R.C., O.P., and J.C.T. contributed new reagents/analytic tools; J.T.H., J.P., N.P., S.S.K., D.B., S.B., V.M.D., and T.M.D. analyzed data; and J.T.H., V.M.D., and T.M.D. wrote the paper.

1. P. L. McGeer, S. Itagaki, B. E. Boyes, E. G. McGeer, Reactive microglia are positive for HLA-DR in the substantia nigra of Parkinson's and Alzheimer's disease brains. *Neurology* **38**, 1285–1291 (1988).
2. M. G. Spillantini *et al.*, Alpha-synuclein in Lewy bodies. *Nature* **388**, 839–840 (1997).
3. N. Panicker, P. Ge, V. L. Dawson, T. M. Dawson, The cell biology of Parkinson's disease. *J. Cell Biol.* **220**, e202012095 (2021).
4. L. A. Volpicelli-Daley, K. C. Luk, V. M. Y. Lee, Addition of exogenous α-synuclein preformed fibrils to primary neuronal cultures to seed recruitment of endogenous α-synuclein to Lewy body and Lewy neurite-like aggregates. *Nat. Protoc.* **9**, 2135–2146 (2014).
5. K. C. Luk *et al.*, Pathological α-synuclein transmission initiates Parkinson-like neurodegeneration in nontransgenic mice. *Science* **338**, 949–953 (2012).
6. R. Cascella *et al.*, The release of toxic oligomers from α-synuclein fibrils induces dysfunction in neuronal cells. *Nat. Commun.* **12**, 1814 (2021).
7. L. A. Volpicelli-Daley *et al.*, Exogenous α-synuclein fibrils induce Lewy body pathology leading to synaptic dysfunction and neuron death. *Neuron* **72**, 57–71 (2011).
8. Y. C. Wong, D. Krainc, α-synuclein toxicity in neurodegeneration: Mechanism and therapeutic strategies. *Nat. Med.* **23**, 1–13 (2017).
9. C. Kim *et al.*, Neuron-released oligomeric α-synuclein is an endogenous agonist of TLR2 for paracrine activation of microglia. *Nat. Commun.* **4**, 1562 (2013).
10. S. G. Daniele *et al.*, Activation of MyD88-dependent TLR1/2 signaling by misfolded α-synuclein, a protein linked to neurodegenerative disorders. *Sci. Signal.* **8**, ra45 (2015).
11. N. Panicker *et al.*, Fyn kinase regulates misfolded α-synuclein uptake and NLRP3 inflammasome activation in microglia. *J. Exp. Med.* **216**, 1411–1430 (2019).
12. A. Sommer *et al.*, Th17 lymphocytes induce neuronal cell death in a human iPSC-based model of Parkinson's disease. *Cell Stem Cell* **23**, 123–131.e6 (2018).
13. C. S. Lindestam Arlehamn *et al.*, α-Synuclein-specific T cell reactivity is associated with preclinical and early Parkinson's disease. *Nat. Commun.* **11**, 1875 (2020).
14. R. Gordon *et al.*, Inflammasome inhibition prevents α-synuclein pathology and dopaminergic neurodegeneration in mice. *Sci. Transl. Med.* **10**, eaah4066 (2018).
15. L. Fellner *et al.*, Toll-like receptor 4 is required for α-synuclein dependent activation of microglia and astroglia. *Glia* **61**, 349–360 (2013).
16. A. Decout, J. D. Katz, S. Venkatraman, A. Ablasser, The cGAS-STING pathway as a therapeutic target in inflammatory diseases. *Nat. Rev. Immunol.* **21**, 548–569 (2021).
17. A. Ablasser *et al.*, cGAS produces a 2′-5′-linked cyclic dinucleotide second messenger that activates STING. *Nature* **498**, 380–384 (2013).
18. K. R. Balka *et al.*, TBK1 and IKKε act redundantly to mediate STING-induced NF-κB responses in myeloid cells. *Cell Rep.* **31**, 107492 (2020).
19. H. Ishikawa, G. N. Barber, STING is an endoplasmic reticulum adaptor that facilitates innate immune signalling. *Nature* **455**, 674–678 (2008).
20. K. J. Mackenzie *et al.*, cGAS surveillance of micronuclei links genome instability to innate immunity. *Nature* **548**, 461–465 (2017).
21. S. Glück *et al.*, Innate immune sensing of cytosolic chromatin fragments through cGAS promotes senescence. *Nat. Cell Biol.* **19**, 1061–1070 (2017).
22. Z. Dou *et al.*, Cytoplasmic chromatin triggers inflammation in senescence and cancer. *Nature* **550**, 402–406 (2017).
23. M. Sharma, S. Rajendrarao, N. Shahani, U. N. Ramírez-Jarquín, S. Subramaniam, Cyclic GMP-AMP synthase promotes the inflammatory and autophagy responses in Huntington disease. *Proc. Natl. Acad. Sci. U.S.A.* **117**, 15989–15999 (2020).
24. X. Song, F. Ma, K. Herrup, Accumulation of cytoplasmic DNA due to ATM deficiency activates the microglial viral response system with neurotoxic consequences. *J. Neurosci.* **39**, 6378–6394 (2019).
25. T.-I. Kam *et al.*, Poly(ADP-ribose) drives pathologic α-synuclein neurodegeneration in Parkinson's disease. *Science* **362**, eaat8407 (2018).
26. W. M. Bonner *et al.*, GammaH2AX and cancer. *Nat. Rev. Cancer* **8**, 957–967 (2008).
27. D. Lingwood, K. Simons, Lipid rafts as a membrane-organizing principle. *Science* **327**, 46–50 (2010).
28. K. Mukai *et al.*, Activation of STING requires palmitoylation at the Golgi. *Nat. Commun.* **7**, 11932 (2016).
29. M. F. Duffy *et al.*, Lewy body-like alpha-synuclein inclusions trigger reactive microgliosis prior to nigral degeneration. *J. Neuroinflammation* **15**, 129 (2018).
30. S. P. Yun *et al.*, Block of A1 astrocyte conversion by microglia is neuroprotective in models of Parkinson's disease. *Nat. Med.* **24**, 931–938 (2018).
31. V. Mathur *et al.*, Activation of the STING-dependent type I interferon response reduces microglial reactivity and neuroinflammation. *Neuron* **96**, 1290–1302.e6 (2017).
32. L. S. Reinert *et al.*, Sensing of HSV-1 by the cGAS-STING pathway in microglia orchestrates antiviral defence in the CNS. *Nat. Commun.* **7**, 13348 (2016).
33. S. Abdisalaam *et al.*, Dysfunctional telomeres trigger cellular senescence mediated by cyclic GMP-AMP synthase. *J. Biol. Chem.* **295**, 11144–11160 (2020).
34. J. D. Sauer *et al.*, The N-ethyl-N-nitrosourea-induced Goldenticket mouse mutant reveals an essential function of Sting in the in vivo interferon response to Listeria monocytogenes and cyclic dinucleotides. *Infect. Immun.* **79**, 688–694 (2011).
35. L. Ahmad, S. Y. Zhang, J. L. Casanova, V. Sancho-Shimizu, Human TBK1: A gatekeeper of neuroinflammation. *Trends Mol. Med.* **22**, 511–527 (2016).

36. T. T. Chu *et al.*, Tonic prime-boost of STING signalling mediates Niemann-Pick disease type C. *Nature* **596**, 570–575 (2021).
37. M. Guo *et al.*, Microglial exosomes facilitate α-synuclein transmission in Parkinson's disease. *Brain* **143**, 1476–1497 (2020).
38. P. d'Errico *et al.*, Microglia contribute to the propagation of Abeta into unaffected brain tissue. *Nat. Neurosci.* **25**, 20–25 (2021).
39. R. E. Marques, R. Guabiraba, R. C. Russo, M. M. Teixeira, Targeting CCL5 in inflammation. *Expert Opin. Ther. Targets* **17**, 1439–1460 (2013).
40. J. Seo *et al.*, Chronic infiltration of T lymphocytes into the brain in a non-human primate model of Parkinson's disease. *Neuroscience* **431**, 73–85 (2020).
41. X. Gui *et al.*, Autophagy induction via STING trafficking is a primordial function of the cGAS pathway. *Nature* **567**, 262–266 (2019).
42. J. A. Oakes, M. C. Davies, M. O. Collins, TBK1: A new player in ALS linking autophagy and neuroinflammation. *Mol. Brain* **10**, 5 (2017).
43. V. Gerbino *et al.*, The loss of TBK1 kinase activity in motor neurons or in all cell types differentially impacts ALS disease progression in SOD1 mice. *Neuron* **106**, 789–805.e5 (2020).
44. H. Yang, H. Wang, J. Ren, Q. Chen, Z. J. Chen, cGAS is essential for cellular senescence. *Proc. Natl. Acad. Sci. U.S.A.* **114**, E4612–E4620 (2017).
45. C. H. Yu *et al.*, TDP-43 triggers mitochondrial DNA release via mPTP to activate cGAS/STING in ALS. *Cell* **183**, 636–649.e18 (2020).
46. D. A. Sliter *et al.*, Parkin and PINK1 mitigate STING-induced inflammation. *Nature* **561**, 258–262 (2018).
47. Y. Hou *et al.*, NAD^+ supplementation reduces neuroinflammation and cell senescence in a transgenic mouse model of Alzheimer's disease via cGAS-STING. *Proc. Natl. Acad. Sci. U.S.A.* **118**, e2011226118 (2021).
48. A. Nazmi *et al.*, Chronic neurodegeneration induces type I interferon synthesis via STING, shaping microglial phenotype and accelerating disease progression. *Glia* **67**, 1254–1276 (2019).
49. A. A. Fatokun, V. L. Dawson, T. M. Dawson, Parthanatos: Mitochondrial-linked mechanisms and therapeutic opportunities. *Br. J. Pharmacol.* **171**, 2000–2016 (2014).